





RESEARCH ARTICLE OPEN ACCESS

Rapid Evolution in Action: Environmental Filtering Supports Coral Adaptation to a Hot, Acidic, and Deoxygenated Extreme Habitat

Carlos Leiva^{1,2}  | Gergely Torda³  | Chengran Zhou (周程冉)^{4,5} | Yunrui Pan (潘云瑞)^{6,7} | Jess Harris³ | Xueyan Xiang (向薛雁)^{4,5} | Shangjin Tan (谭上进)^{4,8} | Wei Tian (田巍)⁹ | Benjamin Hume¹⁰ | David J. Miller^{3,11,12}  | Qiye Li (李启业)^{4,5,8} | Guojie Zhang (张国捷)^{13,14} | Ira Cooke^{11,12}  | Riccardo Rodolfo-Metalpa^{2,15,16}

¹Marine Laboratory, University of Guam, Guam, USA | ²Laboratoire d'Excellence CORAIL, ENTROPIE (UMR9220), IRD, Nouméa, New Caledonia | ³ARC Centre of Excellence for Coral Reef Studies, James Cook University, Townsville, Queensland, Australia | ⁴BGI Research, Wuhan, China | ⁵State Key Laboratory of Genome and Multi-Omics Technologies, BGI Research, Shenzhen, China | ⁶Research Center for eco-Environmental Science, Chinese Academy of Sciences, Beijing, China | ⁷University of the Chinese Academy of Sciences, Beijing, China | ⁸College of Life Sciences, University of Chinese Academy of Sciences, Beijing, China | ⁹BGI-Australia, Herston, Queensland, Australia | ¹⁰Department of Biology, University of Konstanz, Konstanz, Germany | ¹¹College of Public Health, Medical and Veterinary Sciences, James Cook University, Townsville, Queensland, Australia | ¹²Centre for Tropical Bioinformatics and Molecular Biology, James Cook University, Townsville, Queensland, Australia | ¹³Center for Evolutionary & Organismal Biology and Women's Hospital at Zhejiang University School of Medicine, and Liangzhu Laboratory, Zhejiang University Medical Center, Hangzhou, China | ¹⁴Liangzhu Laboratory, Zhejiang University Medical Center, Hangzhou, China | ¹⁵ENTROPIE, IRD, Université de la Réunion, IFREMER, Université de Nouvelle-Calédonie, Nouméa, New Caledonia | ¹⁶Labex ICONA International CO₂ Natural Analogues Network, Tsukuba, Japan

Correspondence: Carlos Leiva (cleivama@gmail.com)

Received: 3 December 2024 | **Revised:** 5 February 2025 | **Accepted:** 5 February 2025

Funding: This work was supported by Australian Research Council Australian Discovery Early Career Award, DE200101064, French Ministère des Affaires Étrangères Government through the Fonds Pacifique, "Adaptation of corals to climate change", Flotte Océanographique Française, National Science Foundation NSF-EPSCoR, OIA-1946352, BGI Australia through the BGI Biodiversity Research, China National GeneBank. Carlos Leiva, Gergely Torda, and Chengran Zhou should be considered joint first author.

Keywords: *Acropora tenuis* | adaptive potential | Bouraké lagoon | genotype–environment associations | ITS2 | natural analogues | natural selection | population genomics | symbiont shuffling | TRPA1

ABSTRACT

The semiencllosed Bouraké lagoon in New Caledonia is a natural system that enables observation of evolution in action with respect to stress tolerance in marine organisms, a topic directly relevant to understanding the consequences of global climate change. Corals inhabiting the Bouraké lagoon endure extreme conditions of elevated temperature (> 33°C), acidification (7.2 pH units), and deoxygenation (2.28 mg O₂ L⁻¹), which fluctuate with the tide due to the lagoon's geomorphology. To investigate the underlying bases of the apparent stress tolerance of these corals, we combined whole genome resequencing of the coral host and ITS2 metabarcoding of the photosymbionts from 90 *Acropora tenuis* colonies from three localities along the steep environmental gradient from Bouraké to two nearby control reefs. Our results highlight the importance of coral flexibility to associate with different photosymbionts in facilitating stress tolerance of the holobiont; but, perhaps more significantly, strong selective effects were detected at specific loci in the host genome. Fifty-seven genes contained SNPs highly associated with the extreme environment of Bouraké and were enriched in functions related to sphingolipid metabolism. Within these genes, the conserved sensor of noxious stimuli TRPA1 and the ABCC4 transporter stood out due to the high number of environmentally selected SNPs that they contained. Protein 3D structure predictions suggest that a single-point mutation causes the rotation of the main regulatory domain of TRPA1, which may be behind this case of natural

This is an open access article under the terms of the [Creative Commons Attribution-NonCommercial-NoDerivs](https://creativecommons.org/licenses/by-nc-nd/4.0/) License, which permits use and distribution in any medium, provided the original work is properly cited, the use is non-commercial and no modifications or adaptations are made.

© 2025 The Author(s). *Global Change Biology* published by John Wiley & Sons Ltd.

selection through environmental filtering. While the corals of the Bouraké lagoon provide a striking example of rapid adaptation to extreme conditions, overall, our results highlight the need to preserve the current standing genetic variation of coral populations to safeguard their adaptive potential to ongoing rapid environmental change.

1 | Introduction

Reef-building corals are the habitat engineers of the most biodiverse marine ecosystem, tropical coral reefs (Knowlton et al. 2010), delivering irreplaceable ecosystem services valued at around nine trillion euros per year to nearly a billion people worldwide (Costanza et al. 2014; Sing Wong et al. 2022). However, anthropogenic climate change jeopardizes these key habitats, with ocean warming, ocean acidification, and seawater deoxygenation representing tremendous threats to coral reefs globally. These harsh conditions are already causing mass bleaching and widespread mortality events, which are predicted to increase in frequency in the following decades and centuries even under the scenario of rapid transition to zero anthropogenic emissions (Calvin et al. 2023). However, with their large effective population sizes and connected populations (Davies et al. 2015; Prada et al. 2016), corals might harbor enough standing genetic variation allowing natural selection to promote tolerant genotypes in the future, with surviving populations rebounding after local bottlenecks (Prada et al. 2016). Additionally, corals possess a plethora of rapid adaptive strategies that could allow them to survive the stressful conditions predicted for the following decades (Torda et al. 2017).

To resolve this dichotomy between the alarming predictions and the evolutionary optimism, it is crucial to understand corals' rapid adaptation and acclimatization mechanisms and their associated consequences. Within this framework, naturally occurring extreme microenvironments that partially mimic the foreseen physicochemical conditions of future oceans (i.e., “natural analogues”) provide unique opportunities to study the biological responses that corals could potentially use to prevail in the Anthropocene (Camp et al. 2018). The fact that corals thrive in these extreme environments suggests that adaptation and/or acclimatization to future ocean conditions is possible. Indeed, recent research on corals from these natural laboratories has unveiled corals' remarkable adaptive strategies and plasticity to cope with extreme conditions, including gene expression regulation (Kenkel et al. 2018; Scucchia et al. 2023), natural selection in coral host genes (Bay and Palumbi 2014; Leiva et al. 2023), and changes in their photosymbiont communities (Camp et al. 2020; Tanvet et al. 2023).

In order to understand the adaptation and acclimatization mechanisms allowing corals to thrive in extreme habitats, we conducted high-coverage (average depth of 67×) genome sequencing on 90 individuals of the reef-building coral *Acropora tenuis* from three localities along a steep environmental gradient in New Caledonia, from the semienclined Bouraké lagoon to a nearby reference reef (Figure 1a–c). To the best of our knowledge, this is the first study sequencing coral whole genomes at high depth from a multi-stressor extreme natural analogue. The three sampling sites represent highly contrasting environments that have been monitored since 2016 (Camp et al. 2017; Maggioni et al. 2021; Tanvet et al. 2022). Extreme conditions in Bouraké have oscillated for at least the last 60 years, likely for centuries, following the tide cycle

in a predictable manner, with daily temperature changes of 6.5°C, variations in dissolved oxygen of 4.91 mg O₂ L⁻¹, and a fluctuating pH between 7.4 and 8.0 (Maggioni et al. 2021) (Figure 1d–f). This extreme fluctuation is due to the semienclined geomorphology of Bouraké that warms up the water that stays in the lagoon during low tide, combined with intense oxidation in the mangrove sediment that acidifies and deoxygenates the water (see Maggioni et al. (Maggioni et al. 2021) for a detailed description of the sites). Although there is no perfect present-day “natural analogue” to future climate conditions, the multi-stressor character of Bouraké partially mimics the multifactorial manifestations of climate change, which is one of the main novelties of our work compared to previous studies from CO₂ seeps (Leiva et al. 2023) or back-reef pools (Bay and Palumbi 2014). Remarkably, our population-level dataset represents an unprecedented opportunity to screen entire coral genomes for signals of natural selection to multiple co-occurring extreme conditions, potentially identifying new molecular mechanisms behind coral adaptation and inferring their adaptive potential to future climate change. Moreover, it provides a framework to study the demographic and diversity consequences associated with strong environmental selection. In addition to genome screening, we also characterized the Symbiodiniaceae communities of sampled coral colonies and described the compositional changes in these microbial associates along the environmental gradients. Symbiodiniaceae is a highly diverse family of dinoflagellates that associate with corals and other marine invertebrates, with different species presenting different capabilities for photosynthetic production, oxidative stress resistance, and thermal stress tolerance (Berkelmans and van Oppen 2006; Cantin et al. 2009; McGinty et al. 2012). Hence, Symbiodiniaceae communities have a prominent role in holobiont fitness, stress resistance, and adaptation. Together, our results show two simultaneous rapid mechanisms to overcome the physiological challenges posed by the extreme Bouraké habitat, describing some of the strategies that reef-building corals may use to survive in the oceans of the future.

2 | Results

A total of 90 colonies of *Acropora tenuis* (identified by colony morphology) were sampled and sequenced from three sites in New Caledonia (Figure 1c), from the surface to 2 m depth compared to mean sea level height. The three sites represent a steep environmental gradient, from the Control site R1 to the Bouraké site B2 (16) (Figure 1d–f). Mean colony sizes were largest at the Bouraké site B2 (54.1 cm ± 20.9 sd) and smallest at Control site R1 (10.9 cm ± 6.17). Three color morphs (brown, cream, and yellow) were present at the Bouraké site B2 and at Control site R2, but only cream and yellow colonies were present at Control site R1. Brown color morphs at Control site R2 were significantly larger in diameter than the other two color morphs at this site (Figure S1).

A total of 2.7 Tb of whole genome sequencing reads were obtained for all samples (Figure S2a). The achieved sequencing

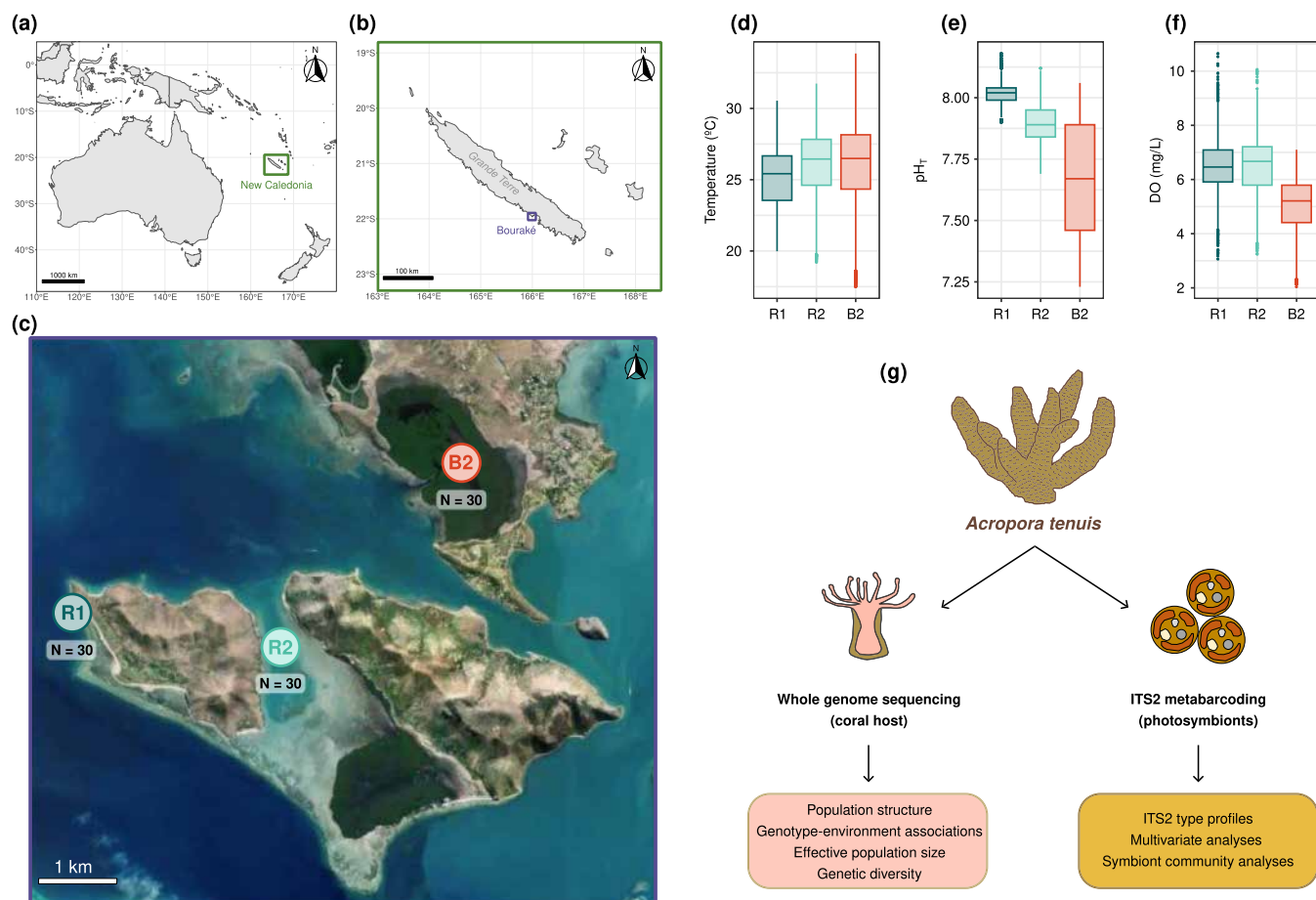


FIGURE 1 | Map and physicochemical characteristics of the study site and overview of the experimental design. (a) Map showing the location of New Caledonia (green square) within the Southwestern Pacific Ocean. (b) Map showing the location of Bouraké (purple square) within New Caledonia. (c) Map of the study area showing the three sampling sites: B2, Bouraké B2; R2, Control site R2; and R1, Control site R1. (d, e, and f) Values of (d) temperature, (e) pH_T, and (f) dissolved oxygen shown by sampling site (Data from Maggioni et al. (Maggioni et al. 2021)). (g) Overview of the experimental design and the analyses performed for each compartment of the coral holobiont. Map lines delineate study areas and do not necessarily depict accepted national boundaries.

depth was over 27× genome-wide, with an average depth of 67×, and the alignment rate was over 0.70 for all but one sample (27× sequencing depth and 0.56 alignment rate for colony 57, Control site R2), and in total approximately 80% of reads could be aligned to the reference genome (Cooke et al. 2020) (Figure S2b). After filtering, 1,709,043 linkage disequilibrium (LD)-pruned SNPs were kept for population genomic analysis. Sample 69 (Control site R1) had 46.14% missing data and was, therefore, removed from downstream analyses. In the remaining 89 samples, missing data accounted for 1.03%. Clonality and phylogenetic analyses revealed the presence of 11 clone clusters (Figures S3 and S4, respectively); hence, we kept only one sample per clone cluster and reconducted the SNP calling and filtering analyses for the remaining 73 samples, keeping 7,894,070 common genome-wide SNPs and 1,722,769 LD-pruned SNPs for downstream analyses.

2.1 | All Coral Colonies Belong to the Same Panmictic Population

Multivariate and clustering analyses of the coral host LD-pruned SNPs revealed that the samples did not cluster by site

of origin. All samples were genetically highly similar and clustered together in the PCA (Figure 2d) and the phylogenetic trees (Figure S4), as well as in the DAPC using the sampling sites as a priori grouping (Figure S5a). The optimal number of ancestral populations in both *snmf* and admixture analyses was one (Figure S5b,c). Admixture results for K2–K6 showed a lack of structure (Figure S5d), supporting the high genetic similarity among all samples.

2.2 | Genotype–Environment Association Analyses Reveal the Targets of Natural Selection in Bouraké

We used the environmental data from Maggioni et al. (Maggioni et al. 2021) to find signals of environmental adaptation to Bouraké in *A. tenuis*. It included 30 environmental variables collected from our study sites between 2017 and 2020, which were summarized into two environmental principal components (ePC). The first ePC (ePC1) explained 71.7% of the total environmental variance and separated Bouraké from the two control sites (Figure 2a). ePC1 summarized information from nearly all variables, outperforming ePC2 in capturing the environmental differences among sampling sites (see PC loadings in Figure S6).

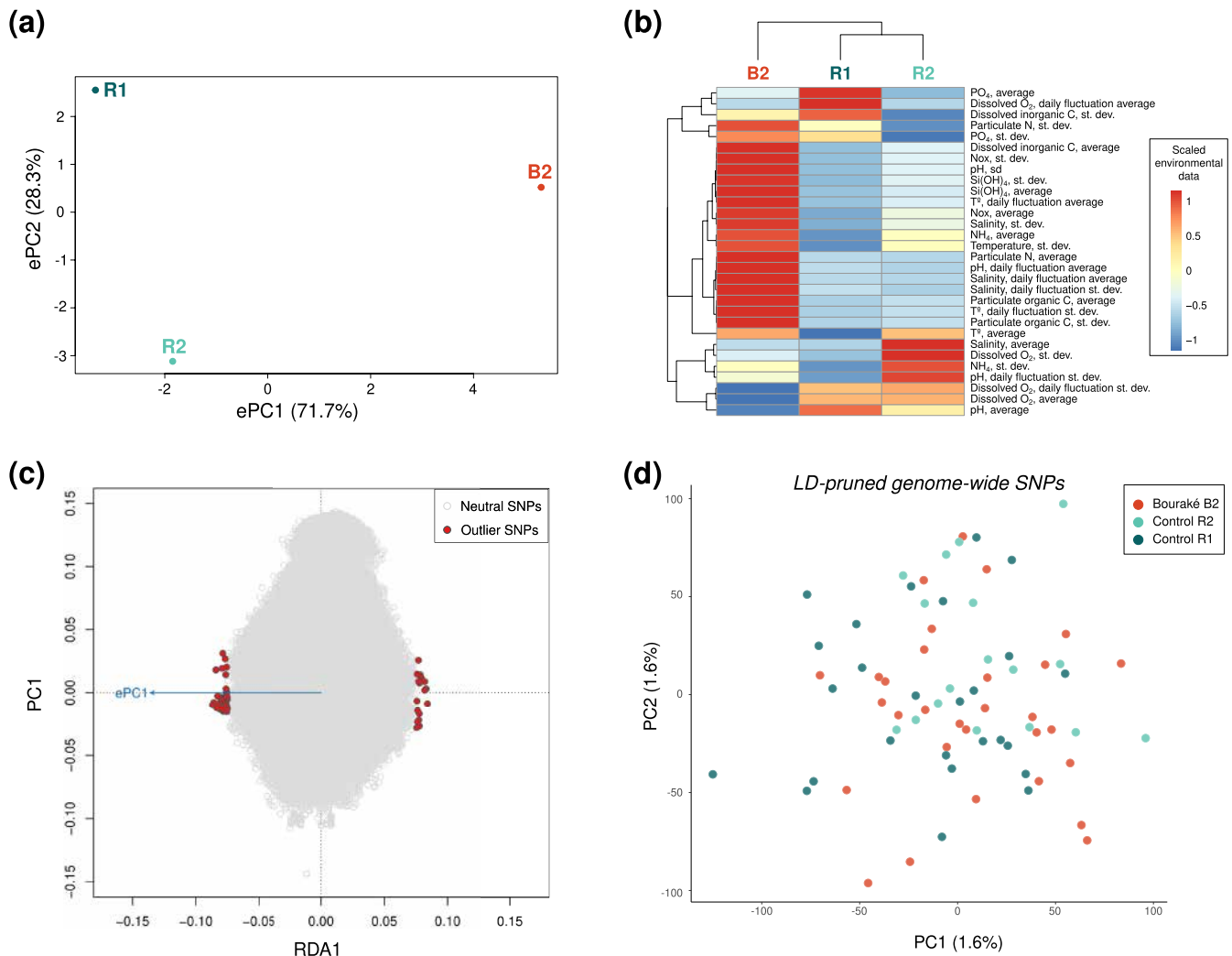


FIGURE 2 | Genotype-Environment association analysis. (a) Environmental PCA results showing the differentiation of the three sampling sites based on the environmental data from Maggioni et al. (Maggioni et al. 2021). (b) Heatmap plot and dendrograms of the scaled environmental data from Maggioni et al. (Maggioni et al. 2021). See environmental matrix in Table S1. (c) RDA space showing the neutral SNPs in gray and the 89 outlier SNPs in red, which were highly associated with the environmental PC1 (ePC1, blue arrow). (d) PCA results using the 1,722,769 LD-pruned genome-wide SNPs.

Most of the environmental variables were highly correlated with Bouraké, including the total average pH (“pH_av”), its total standard deviation (“pH_sd”) and its daily fluctuation (“pH_dd_av”), and the total temperature standard deviation (“T_sd”), its daily fluctuation (“T_dd_av”), and daily standard deviation (“T_dd_sd”) (Figure 2b; see environmental matrix in Table S1).

A redundancy analysis (RDA) detected 89 SNPs that were strongly associated with the ePC1 using a four standard deviations cutoff (Figure 2c). As ePC1 is the PC that differentiated Bouraké B2 from the two control sites (Figure 2a), the SNPs associated with ePC1 are considered candidate SNPs under environmental selection in Bouraké. Contrasting with the lack of population structure using all LD-pruned SNPs (Figure 2d), these 89 SNPs differentiated the Bouraké site from the two reference reefs in a PCA (Figure S7). Functional SNP annotation using SnpEff revealed 57 genes affected by these 89 SNPs associated with Bouraké (Table S2), either having SNPs within the gene body (69 SNPs in 31 genes) or being less than 5 kbp (default value in SnpEff to include the potential effects of SNPs

in gene promoters and enhancers (Cingolani et al. 2012)) from a SNP (26 genes). The enrichment analysis identified seven enriched gene ontology (GO) terms among these 57 genes, with all biological processes related to the sphingolipid metabolism (Table 1). Among the 31 genes with SNPs within their gene body, two stood out as statistical outliers (z-score method, three SD threshold) due to their high number of environmentally associated SNPs. Each of these two genes contained nine of the 89 outlier SNPs identified in the RDA, and both included a missense mutation. One gene, located in Scaffold Sc0000044, was homologous to the human *Transient receptor potential cation channel subfamily A member 1* (*TRPA1*) (blast e-value of 3.3e-90) while the other, located in Scaffold Sc0000025, was homologous to the human *ATP binding cassette subfamily C member 4* (*ABCC4*) (blast e-value of 0). InterProscan searches were performed to validate that both coral protein sequences belonged to the TRPA1 and ABCC4 protein families, respectively (Figures S8 and S9). The rest of the genes had an average of 1.8 SNPs per gene. Genotype frequencies at these 18 SNPs within *TRPA1* and *ABCC4* suggest that two different types of

TABLE 1 | Enriched GO terms among the 57 genes affected by the 89 SNPs highly associated with the environment.

GO term ID	Description	GO Ontology	Gene count, gene set	Gene count, genome background	<i>p</i>	<i>p.adjust</i>	<i>q-value</i>
GO:0016408	C-acyltransferase activity	MF	3	17	6.47e-6	4.49e-3	3.71e-3
GO:0002178	Palmitoyltransferase complex	CC	2	10	2.08e-4	4.78e-2	3.95e-2
GO:0046512	Sphingosine biosynthetic process	BP	2	11	2.54e-4	4.78e-2	3.95e-2
GO:0046520	Sphingoid biosynthetic process	BP	2	12	3.05e-4	4.78e-2	3.95e-2
GO:0006670	Sphingosine metabolic process	BP	2	13	3.59e-4	4.78e-2	3.95e-2
GO:0006684	Sphingomyelin metabolic process	BP	2	15	4.82e-4	4.78e-2	3.95e-2
GO:0046519	Sphingoid metabolic process	BP	2	15	4.82e-4	4.78e-2	3.95e-2

balancing selection are occurring in Bouraké: balancing selection through heterozygote advantage in *TRPA1* (Figure 3a), and balancing selection following a spatially varying selection model across a panmictic population in *ABCC4* (Figure 3f) (Bitarello et al. 2023). These results point to the *TRPA1* and *ABCC4* genes as the main targets of natural selection through environmental filtering in Bouraké, together with a set of genes involved in the sphingolipid metabolism.

To test the putative structural and functional relevance of the environmentally associated missense mutations, we predicted the protein 3D structure of *TRPA1* and *ABCC4* using AlphaFold2 for both the reference and mutated amino acid sequences. The missense mutation Ile920Thr in *TRPA1* is predicted to trigger a relevant structural change in the computationally inferred protein 3D structure, causing a rotation of the TRP helix at the C terminus end of the protein (Figure 3b,e). This is supported by a low structural consistency in the area surrounding the mutation (Figure 3c) and low pairwise interatomic distance consistencies in the TRP helix (Figure 3d). Contrastingly, the missense mutation Ser282Cys in *ABCC4* is predicted to occur in the cytoplasmic extreme of the transmembrane helix four (TM4) and does not seem to cause any structural change in its alpha helix secondary structure (Figure 3g). Regions of low structural and interatomic distance consistencies (Figure 3h,i) correspond to low confidence areas in the protein models, which do not appear to be related to the environmentally associated mutation (Figure 3j).

The putative heterozygote advantage in the *TRPA1* gene was formally tested with Hardy–Weinberg equilibrium (HWE) tests. For all nine SNPs showing signals of environmental selection in *TRPA1*, the observed number of heterozygotes was higher than expected under HWE, while the number of alternative homozygotes was lower than expected (Table S3). This supports the hypothesis of heterozygote advantage and alternative

homozygote lethality. However, different SNPs and different significance tests yielded contrasting results. For two SNPs, the differences between observed (0/0: 15, 0/1: 15, 1/1: 0) and expected (0/0: 17, 0/1: 11, 1/1: 2) genotype frequencies were statistically significant using a Likelihood ratio test (*p* value = 0.02) and marginally significant using a chi-square test (*p* value = 0.07) (Table S3). For the remaining seven SNPs, no significant differences were found between observed (0/0: 19, 0/1: 15, 1/1: 0) and expected (0/0: 20, 0/1: 9, 1/1: 1) genotype frequencies with either test (Likelihood ratio test *p* value = 0.11, chi-square test *p* value = 0.22) (Table S3). The ternary plot illustrates the position of the two SNPs that showed statistical significance, as well as the position of the other seven SNPs, which are closer to the HWE parabola (Figure S10).

2.3 | Plastic Acclimatization Response via Symbiodiniaceae Communities

The Symbiodiniaceae communities of the coral samples from the three study sites were all exclusively composed of *Cladocopium* spp., and no other Symbiodiniaceae genera were detected in our samples. The NMDS of the ITS2 sequence abundance data (following a Wisconsin double standardization and 4th square-root transformation) showed that Bouraké and the Control site R2 were relatively similar, while Control R1 was substantially different (Figure 4a). The *Cladocopium* sequences that drove the differentiation of Bouraké samples from both control sites were C1cb, C1br, C1bh, 63347_C, and 21039_C, as detected by simpler analyses (Figures S11a and S12). Of these sequences, 63347_C was completely absent from both Controls, while C1cb and 21039_C were completely absent from Control R1 (Figure S11b) and were three and four times more abundant in Bouraké than at Control site R2, respectively (Figure S13a). Control site R1 was characterized by the presence of *Cladocopium* species that were absent from Bouraké, such as members of the C50 group (C50f, C50w,

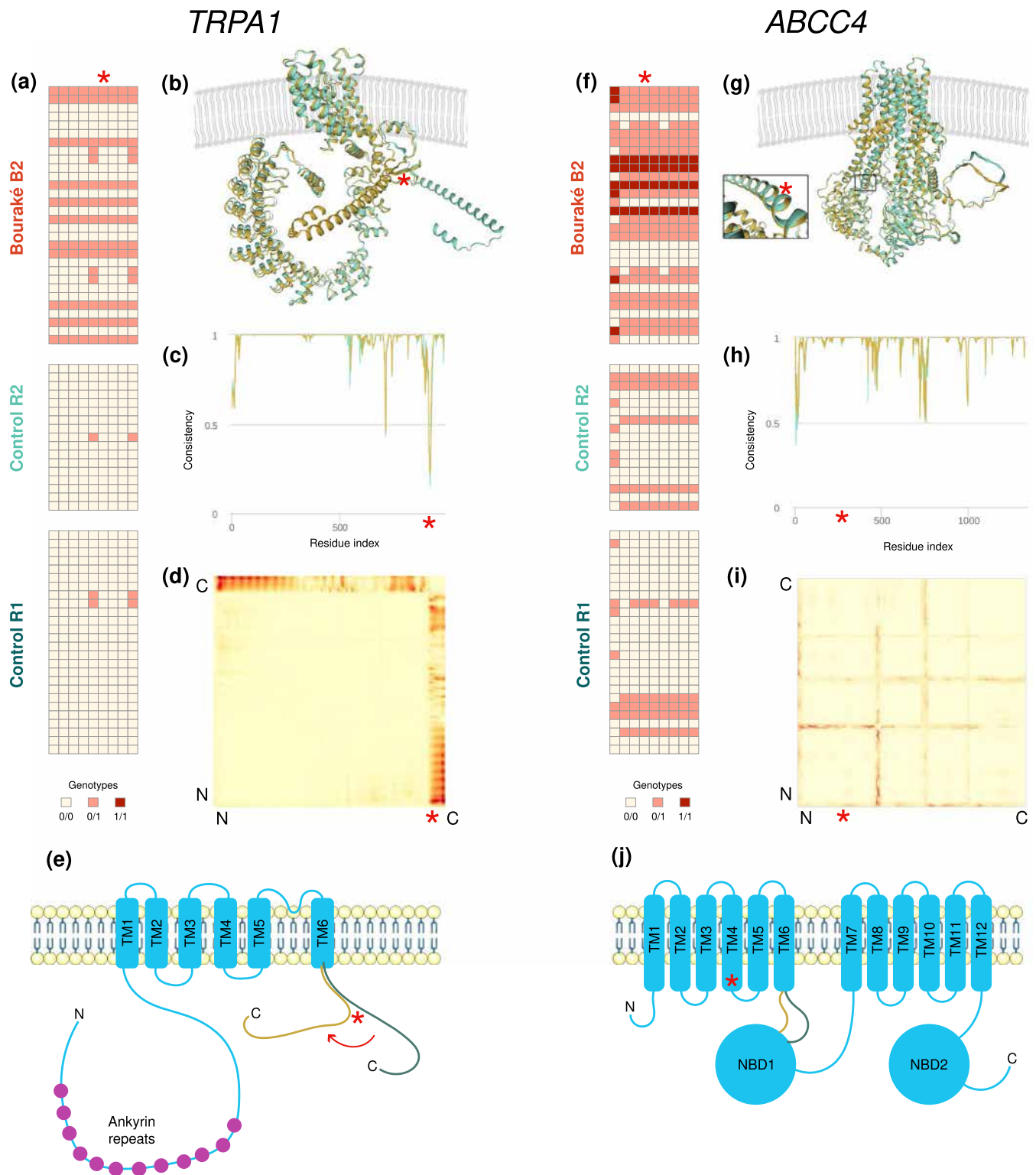


FIGURE 3 | Legend on next page.

C50p, C50a), the C3 group (C3bm, C3b), and several others (Figure S9b). These same ITS2 sequences were present in low abundance in Control site R2 (Figure S13b).

Symbiodiniaceae alpha diversity decreased following the environmental gradient from the least disturbed to the most extreme site: Control R1, seven profiles; Control R2, three profiles; Bouraké, one profile (Figure 4b). The only ITS2 profile found

at Bouraké, C1-C1b-C1c-C42.2-C1br-C1bh-C1cb-C72k-C3, was also present at Control R2 (Figure 4b).

2.4 | The Consequences of Rapid Adaptation

To test for possible demographic and diversity consequences of rapid adaptation at the holobiont level, we inferred recent

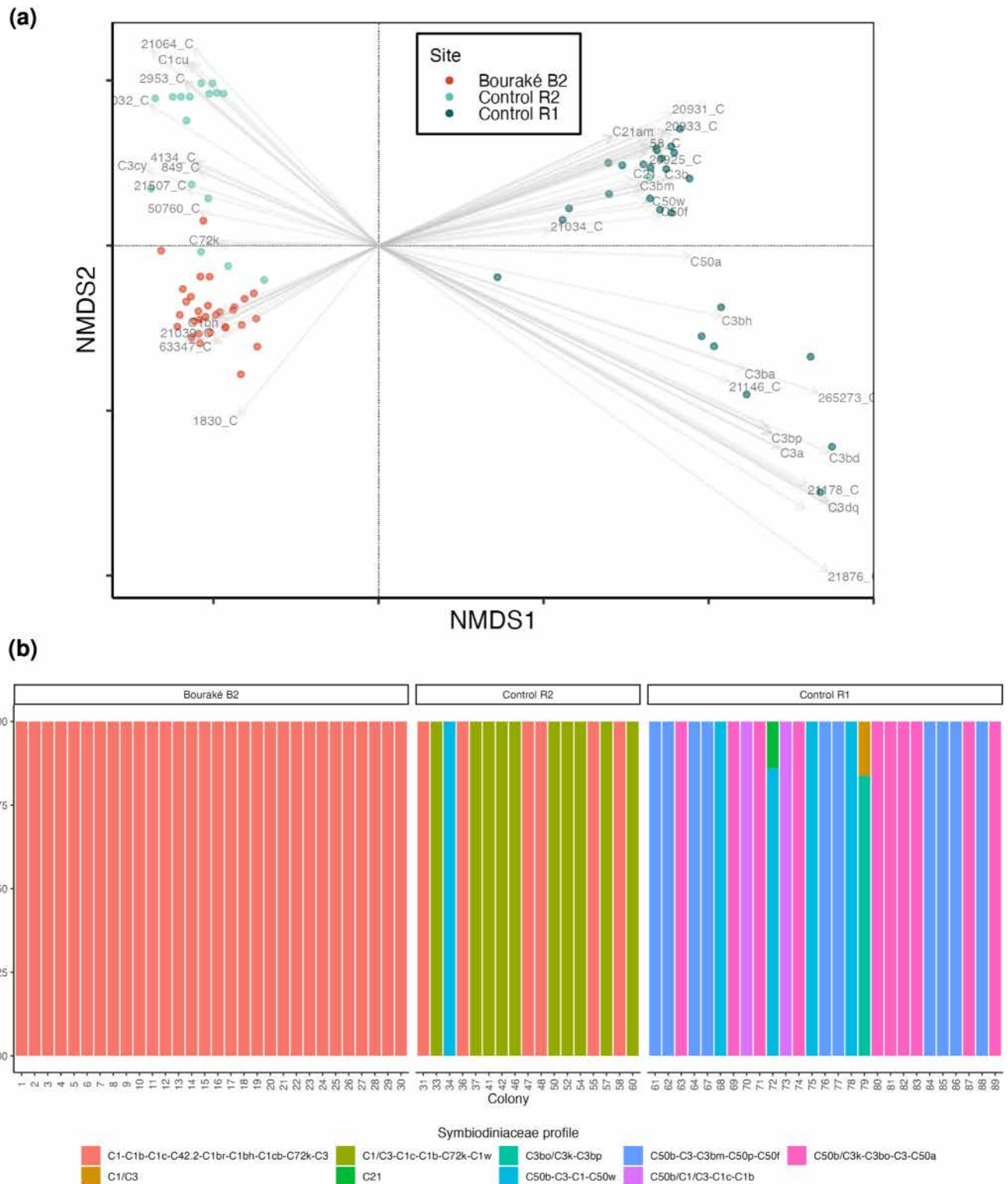
FIGURE 3 | Genotype frequencies and predicted protein 3D structural effects on the two main targets of natural selection through environmental filtering in Bouraké, TRPA1 (a–e) and ABCC4 (f–j). (a) Genotype frequencies of the nine environmentally associated SNPs found in TRPA1. Each row represents an individual and each column represents a SNP. Red asterisk represents the missense mutation Ile920Thr in (a–e). (b) predicted 3D structure models for both reference (green) and mutated (gold) TRPA1 proteins. (c) Structural consistency between reference and mutated TRPA1 predicted proteins. (d) Pairwise interatomic distance consistencies between reference and mutated TRPA1 predicted proteins. Yellow indicates high consistency, while red indicates low consistency areas. (e) Model for the effects of the Ile920Thr missense mutation in TRPA1. (f) Genotype frequencies of the nine environmentally associated SNPs found in ABCC4. Each row represents an individual and each column a SNP. Red asterisk represents the missense mutation Ser282Cys in (f–j). (g) predicted 3D structure models for both reference (green) and mutated (gold) ABCC4 proteins. The inset shows the position of the missense mutation. (h) Structural consistency between reference and mutated ABCC4 predicted proteins. (i) Pairwise interatomic distance consistencies between reference and mutated ABCC4 predicted proteins. Yellow indicates high consistency, while red indicates low consistency areas. (j) Model for the effects of the Ser282Cys missense mutation in ABCC4.

effective population sizes (N_e) and genetic diversities for the coral populations and compared Symbiodiniaceae alpha diversity among the three different sampling sites. The reconstruction of recent N_e showed that the samples from Bouraké present a current N_e an order of magnitude lower than the colonies from the Controls R1 and R2 (Figure 5a). Both Control sites experienced a population contraction during the Little Ice Age (~1450–1850 CE), followed by demographic expansions to reach the current N_e values of ~173,000 individuals in R1 and ~830,000 individuals in R2. However, the Bouraké samples present a current N_e of only ~34,000 individuals (Figure 5a). Genetic diversity measured as nucleotide diversity (π) was significantly different among sampling sites (Welch one-way test, p value = 1.573×10^{-8}) and between each pairwise comparison (Mann–Whitney U test, p values < 1×10^{-8}), with Bouraké presenting the lowest genetic diversity ($\pi = 0.00193 \pm 0.000394$), Control site R1 an intermediate value ($\pi = 0.00998 \pm 0.00651$), and Control site R2 the highest nucleotide diversity ($\pi = 0.0470 \pm 0.0273$) (Figure 5b).

3 | Discussion

Whether corals' adaptation and acclimatization mechanisms can occur fast enough to cope with climate change will be key to the persistence of coral reefs in the Anthropocene. Here, we identified two rapid strategies that *Acropora tenuis* colonies from Bouraké, a semi-enclosed lagoon in New Caledonia, employ to thrive in a harsh environment that partially mimics the foreseen physicochemical conditions of future oceans. The newly sequenced whole genomes of *A. tenuis* from New Caledonia were all similar from a population genetic point of view using the whole genome sequences, indicating that all corals belonged to the same panmictic population. This was supported by all analyses performed. Given the pervasive prevalence of cryptic coral lineages within *Acropora*, analyses to determine that all samples belong to the same lineage/species are crucial for population genomic studies. Despite constituting a panmictic population, a few genes enriched in sphingolipid metabolism functions appeared highly associated with the Bouraké extreme environment, a signal of natural selection through environmental filtering (Capblancq and Forester 2021). Sphingolipids are involved in many cellular physiological functions in cnidarians, including the heat stress response (Kitchen and Weis 2017) and the regulation of cnidarian–dinoflagellate symbiosis (Detournay and Weis 2011). Among these genes associated with Bouraké, two genes with homology to human *TRPA1* and *ABCC4* stood out due to the significantly high number of environmentally

associated SNPs that they presented. Although further experimental validation of our predicted proteins is needed, protein 3D structure models showed that the missense mutation identified in *TRPA1* provokes a significant structural change in the inferred protein 3D structure, causing the rotation of one of the main regulatory domains of *TRPA1*, the C-terminal TRP helix (Zhao et al. 2020). This is particularly relevant because *TRPA1* is a transmembrane ion channel extensively characterized in many animal species, including cnidarians, as a sensor of pain, temperature, environmental irritants, and O_2 (Mori et al. 2017; Peng et al. 2015; Russo 2019). In *Acropora* corals, *TRPA1* is significantly more expressed at noon than at night (Bertucci et al. 2015) and is upregulated early in the infection of coral larvae with Symbiodiniaceae (Mohamed et al. 2016; Yoshioka et al. 2021). Given its role in O_2 sensing and symbiosis, coral *TRPA1* is probably involved in ROS sensing, which might be behind its selective pressure in Bouraké. Remarkably, single-point mutations in the C-terminal TRP helix modify the voltage and chemical sensitivity of human *TRPA1* (Samad et al. 2011). Our results suggest that this mutation causes a structural change in *TRPA1* that might be maintained by balancing selection in Bouraké, suggesting a model of heterozygote adaptive advantage in the extreme habitat. Genotype frequencies in *TRPA1* mirror the classic example of balancing selection in humans, the high frequency of the sickle-cell hemoglobin allele HbS in malaria endemic regions due to the heterozygote advantage against fatal malaria and the alternative homozygote lethality (Aidoo et al. 2002). Indeed, genotype frequencies in the *TRPA1* gene show an excess of heterozygotes and a dearth of alternative homozygotes compared to the expected genotype frequencies under HWE, providing some support for the hypothesis of heterozygote advantage and alternative homozygote lethality. However, these differences are only statistically significant for two of the nine SNPs in *TRPA1*, with the results varying depending on the statistical test used. These contrasting outcomes suggest that the small sample size may limit the statistical power of the tests, preventing definitive conclusions. Regarding *ABCC4*, although the missense mutation did not cause any structural change in the protein, any of the other eight intronic and synonymous variants could explain the selective pressure identified in this gene, as they can also impact fitness through, for instance, mRNA splicing disruption and gene expression regulation (Bailey et al. 2021). The *ABCC4* transporter participates in detoxification and chemical protection in cnidarians (Goldstone 2008), and was found upregulated in corals from the polluted waters of the Port of Miami, Florida, USA (Rubin et al. 2021). Our results indicate that there is a mixed larval pool



shared between environments that are severely filtered by environmental selection in Bouraké, similar to the adaptation of *Acropora hyacinthus* to a highly variable back-reef pool in Ofu Island, American Sāmoa (Thomas et al. 2018). Our results suggest that the environmental filtering in Bouraké selects specific genotypes from the shared larval pool that are able to tolerate

the extreme environment, and hence, are genetically preadapted to the Bouraké extreme habitat. Given the high coral recruitment rates in Bouraké (Tanvet et al. 2022), this environmental filtering is most likely acting on young recruits. However, the precise stage in their lifespan when this filtering occurs remains unclear.

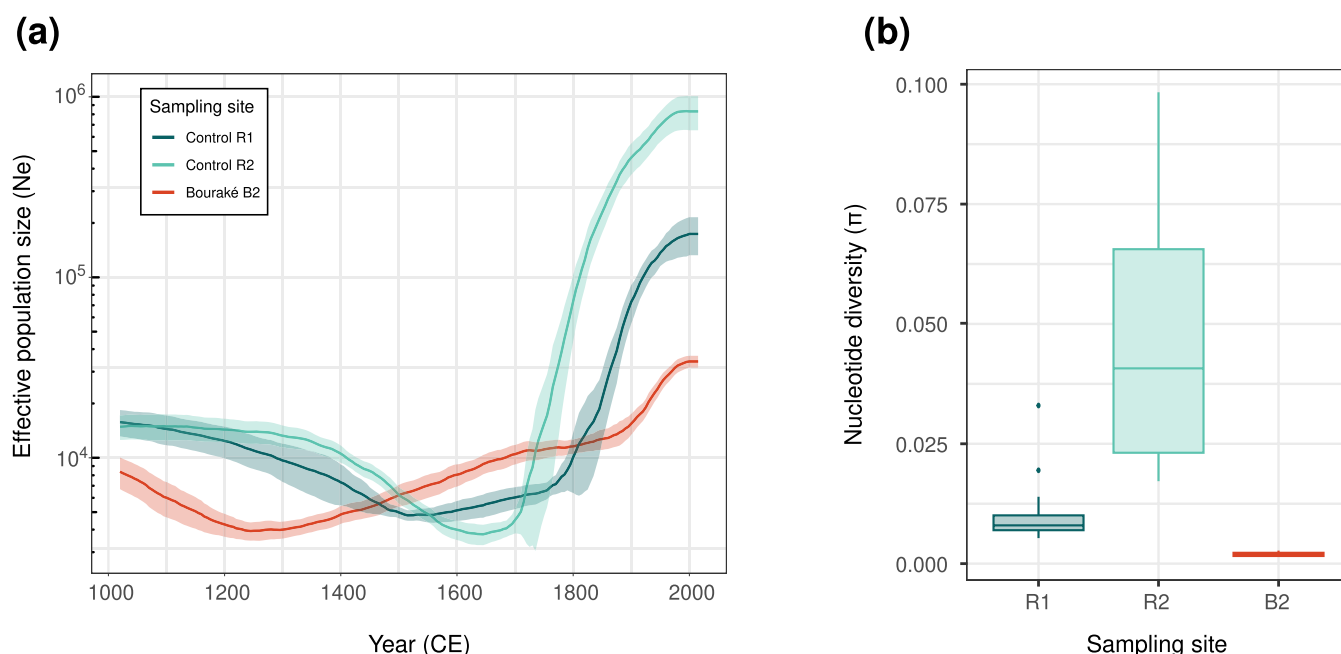


FIGURE 5 | Consequences of rapid adaptation in the coral host. (a) Effective population size (N_e) estimation per sampling site for the coral host. The plot shows the last 200 generations, equaling 1000 years using a generation time of 5 years. (b) Nucleotide diversity (π) per sampling site for the coral host.

The lack of genetic differentiation among corals from the three study sites implies that this is a rapid adaptation response, occurring within a panmictic population potentially even in a single generation. Our results indicate that larvae are freely moving across our study area, and the adult coral colonies collected from Bouraké are likely recruits from a mixed larval pool from the three sites. The high-standing genetic variation in the panmictic population provides the raw material for natural selection to act upon, specifically through environmental filtering at the Bouraké B2 site. Examples of genomic adaptation in a single generation have been found in a handful of study systems, such as in Darwin finches (Boag and Grant 1981) and in green anole lizards (Campbell-Staton et al. 2017). Our results are in line with recent studies showing the rapid adaptive potential of corals to a diversity of extreme microenvironments that partially overlap with future ocean conditions (Bay and Palumbi 2014; Fuller et al. 2020; Leiva et al. 2023; Thomas et al. 2022), suggesting that at least some coral species might be able to cope with rapid environmental change. Contrastingly, other studies found that the locally adapted coral populations were also genetically differentiated across different spatial scales (Scucchia et al. 2023; Smith et al. 2022; Zhang et al. 2022), alerting that compositional changes in coral assemblages can be expected in the near future due to the spectrum of adaptation strategies that coral species employ. Interestingly, rapid adaptation has been exclusively found in species of the genus *Acropora* (Bay and Palumbi 2014; Fuller et al. 2020; Leiva et al. 2023; Thomas et al. 2022), which also possesses genomic strategies that might have helped them adapt, diversify, and thrive globally (Shinzato et al. 2021). This suggests that although *Acropora* species are highly vulnerable to bleaching, postbleaching mortality, and often succumb to environmental stressors (Hughes et al. 2018; Ortiz et al. 2021), some fast-growing and reef-building *Acropora* species possess swift adaptive capabilities that may help them cope with rapid environmental change.

Besides signals of rapid adaptation in the coral host genome, we also found distinct Symbiodiniaceae communities at each sampling site, in agreement with previous studies in Bouraké using different coral species (Camp et al. 2020; Tanvet et al. 2023). This points to an acclimatization response to the stressful Bouraké habitat, as recently found for *Acropora muricata* colonies that survived a bleaching event in Bouraké by shuffling their original Symbiodiniaceae to heat-tolerant ones (Alessi et al. 2024). Indeed, the symbiotic algal community of corals has long been known to greatly influence their thermal tolerance (Baker et al. 2004), and its composition is largely determined by the environment (Quigley et al. 2017). This acclimatization response via Symbiodiniaceae communities was not found in other *Acropora* species in similar contexts of local adaptation across spatially contrasting habitats (Thomas et al. 2022; Zhang et al. 2022), highlighting the wide diversity of acclimatization responses that closely related corals may use. Moreover, we detected a reduced Symbiodiniaceae type diversity in Bouraké, suggesting that a single symbiont species is selected there due to its better performance under extreme conditions. However, due to species-specific trade-offs in coral-symbiont relationships (Abrego et al. 2008), there is not a single best-suited symbiont species for surviving the same extreme conditions across coral species. For instance, *A. tenuis* in this study and *A. muricata* in Alessi et al. (Alessi et al. 2024) are both associated with C1 *Cladocopium* species, while *Acropora pulchra* and *Porites lutea* host A1 *Symbiodinium* and C15 *Cladocopium* species in Bouraké, respectively (Camp et al. 2020). These discrepancies emphasize a potentially important pitfall of heat-evolved algal symbiont studies: It is unlikely that a single heat-evolved symbiont species could improve stress resilience/resistance in different coral species. This is added to the costs and potential risks of breeding and inoculating heat-evolved symbionts and releasing them into the wild (Anthony 2016), when, actually, species-specific symbionts that have been evolving for centuries

or even millennia in multi-stressor conditions are already found in natural extreme habitats such as Bouraké. Besides the two rapid adaptive responses found here, other mechanisms might contribute to the adaptive potential of corals to climate change, such as a transgenerational plasticity through epigenetic modifications, the effects of the bacterial microbiome, or the interactions among all holobiont partners (Torda et al. 2017).

Although our results bring some optimism by revealing two simultaneous rapid adaptive responses to an extreme environment, they also show the demographic and diversity impacts of natural selection in the Bouraké population. We found that the effective population size and the nucleotide diversity were one order of magnitude lower in Bouraké compared with the Control sites, in line with recent findings in species in selective breeding programs (Saura et al. 2021). Despite coral larvae freely moving among sites, the strong environmental filtering in Bouraké reduces genetic diversity and effective population size at that particular site, which is expected under a model of natural selection with gene flow (Sork 2016; Wang et al. 2016). The fact that the Control site R2 presented the highest genetic diversity suggests links to the intermediate disturbance hypothesis (Connell 1978), as shown for the marine benthic communities of a CO₂ seep system at La Palma Island (Canary Islands, Spain) (González-Delgado et al. 2023). Contrastingly, Symbiodiniaceae communities did not follow a pattern concordant with the intermediate disturbance hypothesis, as the Control site R1 presented the highest alpha diversity. Nevertheless, the Bouraké site presented the lowest diversity values in both analyses, suggesting that although corals might have the ability to promptly adapt to future ocean conditions via the rapid adaptive mechanisms outlined above, among others, the associated population bottlenecks could result in the loss of diversity in both the coral host and its symbiotic microbial community, with potential detrimental impacts. Moreover, together with previously identified trade-offs in diversity and growth (Scucchia et al. 2023), our results emphasize the need for caution when considering the use of these locally adapted corals or synthetically enhanced corals for restoration plans. Finally, in line with the photosymbiont results from Hume et al. (Hume et al. 2016), our results highlight the importance of maintaining a high-standing genetic variation in order to safeguard corals' rapid adaptive potential, which should be translated into spatial conservation programs ensuring the protection of a wide diversity of habitats and populations.

4 | Materials and Methods

4.1 | Study Sites and Sample Collections

Thirty colonies of the reef-building scleractinian *Acropora tenuis* were sampled at each of three sites in New Caledonia, within a few kilometers from each other (Figure 1c) in March 2020 on board R/V Alis as part of the Supernatural Oceanographic Cruise (<https://doi.org/10.17600/18001102>). The three sites were chosen because they had highly contrasting environments, which have been monitored since 2016 (Camp et al. 2017; Maggioni et al. 2021; Tanvet et al. 2022). Here, we collected corals from the same sites that were used in such previous studies, and for which detailed physical and chemical descriptions were reported. Briefly, the semiencllosed bay of Bouraké is a shallow

lagoon (5 m depth) surrounded by mangrove forests, with seawater pH, dissolved oxygen, and temperatures that regularly fluctuate, reaching, respectively, minimum values of 7.23 pH units, 2.28 mg O₂ L⁻¹, and a maximum of 33.85°C (Table S1). The environmental variability in the oxygen, temperature, and pH in Bouraké is directly related to the tidal cycle, with changes in a single day of up to 4.91 mg O₂ L⁻¹, 6.50°C, and 0.69 pH units (Maggioni et al. 2021). Despite the extreme environmental conditions, 66 species of scleractinian corals have been identified in Bouraké, forming an abundant and diverse reef that is similar to the reefs found at the two control sites R1 and R2. The lagoon's geomorphology has been unchanged for at least 80–100 years (Maggioni et al. 2021), probably more, meaning that several generations of corals have experienced extreme conditions. Coral colonies were identified in situ as *Acropora tenuis* based on Veron 2000. As New Caledonia was not included in the recent taxonomic revision of *A. tenuis* (Bridge et al. 2024), we decided to keep the name *A. tenuis* for our samples, given their proximity to the *A. tenuis* type locality in Fiji. Samples were photographed and geotagged using an Olympus Tough TG5 camera synchronized to a Garmin eTrex10 surface GPS buoy. Two nubbins approximately 2 cm in length were broken off the colonies using a dive knife and conserved in absolute ethanol, then stored at –20°C until processing. All fieldwork, specimen collection, and experimental procedures were conducted in compliance with ethical standards and with the approval of the relevant authorities, including sample collection permits (No. 3413–2019), CITES export and import permits (No. FR2098800026-E, PWS2020-AU-001254, 2020CN/IC001674/GZ), and institutional ethical clearance (Ethics Approval No. BGI-IRB E21057, No. FT 19060).

4.2 | DNA Extraction, Library Preparations, and Sequencing

A modified version of a salt precipitation-based extraction method developed for shrimp tissues (Wilson et al. 2002) was used to extract DNA from the coral holobiont tissue. DNA extracts were quality checked on a Nanodrop and Qubit fluorometer. Sequencing libraries were constructed with an average insert size of 400 bp at BGI-Shenzhen and the whole genome sequencing was done on the DNBSEQ platform (MGI Tech Co., Shenzhen, China) with a 100 bp paired-end (PE100) sequencing strategy following the manufacturer's protocol (Huang et al. 2017). Over 10Gb sequencing data were generated for each sample and reads were then filtered using SOAPnuke v2.1.1 (Chen et al. 2018) with the following parameters “-n 0.1 -q 0.5 -l 12 -M 2.” In detail, low-quality reads were removed if they met one or more of the following criteria: (1) an N-content of more than 10%; (2) the presence of adapter contamination (reads overlapping more than 50% with the adapter sequence, with a maximal 2 bp mismatches to the adaptor sequence); or (3) more than 50% of the read length below Q12.

The ITS2 region was separately sequenced to accurately characterize the Symbiodiniaceae community of the coral holobiont samples. We used ITS2 forward (5'-TCGTCGGCAGCGT CAGATGTGTATAAGAGACAGGTTGAATTGCAGAACTCC GTG-3') and ITS2 Reverse (5'-GTCTCGTGGGCTCGGAGAT GTGTATAAGAGACAGCCTCCGCTTACTTATATGCTT-3')

Illumina-tagged primers from Hume et al. (Hume et al. 2018) to amplify the ITS2 gene using DreamGreen PCR master mix (ThermoFisher Cat no. K1081) for a total of 35 PCR cycles. Library preparation and amplicon sequencing (MiSeq 150bp Paired-end) were carried out at the Ramaciotti Centre for Genomics (UNSW Sydney). Coral colonies that were identified as clones were removed from these analyses to avoid potential biases due to the impact of host genotype on the symbiont community.

4.3 | Genome Alignment and SNP Calling

Firstly, sequence reads were aligned to the *Acropora kenti* published reference genome (genome size: ~0.48 Gb) (Cooke et al. 2020) with BWA-MEM using Sentieon (v202010) (Sentieon Inc) with default parameters. This genome was chosen because at the outset of this study, *A. kenti* was synonymized with *A. tenuis* and this species is likely to represent the most closely related high-quality genome reference. SNP calling was performed for each individual according to the Broad Institute's best practices pipeline: Mark duplications, Indel realignment, base quality score recalibration, and genome vcf (GVCF) calling, implemented by Sentieon. All 90 GVCF files were then combined and genotyped by Sentieon's GVCFTyper with a minimum confidence threshold of 30 for both calling and emitting variants, restricted to a maximum of two alternative alleles. SNPs and indels were extracted using GATK (v4.2.0.0) SelectVariants, with subsequent indel filtration based on quality depth and mapping quality. After that, low-confidential variants were removed using GATK VariantFiltration and VCFtools (v0.1.15) based on criteria encompassing a minimal quality score of 30, a minimal mapping quality of 40 while also setting a minimum minor allele frequency of 0.05, and a maximum missing rate of 0.1. After this, the Linkage Disequilibrium-pruned VCF file for 90 samples was obtained using PLINK (v1.9) (Chang et al. 2015) with the following criteria: (1) sites with a *p* value of deviation from Hardy-Weinberg Equilibrium test below 0.001 excluded; and (2) to assess population structure, we used LD-pruning to detect the variants in approximate linkage equilibrium using "--indep-pairwise 50 10 0.5" and filtered out these variants from the final VCF file (This command is to calculate pairwise LD within a 50 SNP window and remove one SNP from a pair where the LD exceeds 0.5 before moving on 10 SNPs and repeating the procedure). The missingness on a per-individual basis was generated using VCFtools (v0.1.16) (Danecek et al. 2011) "--missing-indv" and plotted using R ggplot2.

Initial data exploration showed that one sample (id 69) had a high proportion of missing data (46.14%, compared to the average of 1.03%) and therefore, had to be excluded from downstream analyses. Additionally, in order to detect potential clones, relatedness indices between pairs of colonies were calculated using VCFtools "--relatedness2." A threshold of 0.35 was used to identify clones (Manichaikul et al. 2010), revealing the existence of 11 clone clusters, mostly from the Control site R2 (Figure S3a). These results were verified with an Identity-By-State (IBS) analysis using the function "snpgdsIBS" of the SNPRelate R package (Zheng et al. 2012) (Figure S3b). Hence, we removed sample id 69, kept only one sample per clone cluster, and repeated the genotyping and filtering analyses for the remaining 73 samples,

resulting in a total of 7,894,070 common genome-wide SNPs and 1,722,769 LD-pruned SNPs for downstream analyses. The final number of samples for each population is, therefore, Bouraké B2: 30, Control site R2: 17, Control site R1: 26.

4.4 | Population Genetic Structure

The vcf file of the nonclonal LD-pruned SNP dataset was inputted into the R environment and transformed to a genlight object using the "read.vcfR" and "vcf2genlight" functions from the VCFR (v.1.14.0) R package (Knaus and Grünwald 2017), respectively. A principal component analysis (PCA) was performed using the "glPca" function in the adegenet (v.2.1.7) R package (Jombart 2008), and plotted using ggplot2 (v.3.4.3) (Wickham and Wickham 2016). A discriminant analysis of principal coordinates (DAPC) was run using the "dapc" function in adegenet with the sample site as a grouping. Admixture coefficients per sample were estimated using the "snmf" function in the LEA (v.3.12.2) R package (Frichot and François 2015), with the ancestral populations ranging from 1 to 15 ("K=1:15") and 10 repetitions per K ("repetitions=10"). Additionally, we ran ADMIXTURE (v.1.3.0) (Alexander et al. 2009) with the cluster number K ranging from 1 to 7 and 100 replicates per K. The most probable K value was determined by cross-validation ("cv" flag). One randomly selected result from the 100 replicates for each K was plotted using the ggplot2 R package.

4.5 | Phylogenetic Analyses

Phylogenetic analyses were run separately for the nuclear and the mitochondrial genomes. For the nuclear genome, SNP data were subsampled to fall only on exons, introns, genes, or non-genes using BCFtools (v.1.8) (Danecek et al. 2021) and BEDTools (v.2.30.0) (Quinlan and Hall 2010), and these subcategories were first analyzed separately. SNP datasets from the different regions were converted to Phylip format using vcf2phylip (v.2.7) (Ortiz 2019). Phylogenetic trees were then inferred using IQtree (v.2.1.3) (Minh et al. 2020) with parameters "--m GTR+ --seqtype --runs 2 -B 5000" and plotted using iTOL (v.5) (Letunic and Bork 2021) with sample 69 as an outgroup.

For the mitochondrial, reads were mapped to the mitochondrial reference genome (NCBI accession number: NC.003522) using Sentieon bwa mem, and the mitogenomes consensus sequences were called with commands following Cooke et al. (Cooke et al. 2020) using SAMtools and BCFtools. Mitochondrial genomes were then aligned using Mafft (v.7.313) (Katoh 2002) and trimmed using MEGA6 (Tamura et al. 2013). The mitochondrial phylogenetic tree was inferred using IQtree with a GTR substitution model and plotted using iTOL.

4.6 | Demographic History and Genetic Diversity

Recent variations in effective population size were estimated per sampling site using the Genetic Optimization for Ne Estimation (GONE) (Santiago et al. 2020). First, a pseudo-chromosome-level genome was achieved by employing the RagTag tool (Alonge et al. 2022) with a chromosome-level genome of

Acropora millepora (v2.01) as the reference dataset following the guidance. The use of this approach is supported by the highly conserved synteny in Scleractinian genomes (He et al. 2024) and has been previously used by Zhang et al. (Zhang et al. 2024) using the same *Acropora* species. However, a chromosome-level reference genome for *Acropora tenuis* could certainly improve our demographic history inference. The vcf file and the gff file were then converted to chromosome-mapped files according to the RagTag coordinates file. One vcf file per sampling site was then generated with BCFtools (v1.10) using the chromosome-level vcf file obtained from RagTag, which were then converted to plink ped and map format files using PLINK v1.9. The GONE software was run 20 times for each sampling site, with each run taking a new subsample of 50,000 SNPs per chromosome (“maxNSNP=50,000”) to calculate confidence intervals. Each simulation was run with 40 internal replicates (“REPS=40”) for 2000 generations (“NGEN=2000”) in 400 bins (“NBIN=400”), with a maximum recombination rate of 0.05 (“hc=0.05”), and using the “unknown phase” option (“PHASE=2”). Results were plotted with ggplot2 using a generation time of 5 years (Cooke et al. 2020; Thomas et al. 2022).

Genetic diversity measured as nucleotide diversity (π) was calculated for each sampling site using the formula $\pi = 2 \times N_e \times \mu$ (Charlesworth 2009; Khatri and Burt 2019) and the N_e values from the most current generation from each of the 20 runs per site. Differences among groups were first tested with an ANOVA, using the aov function in R, followed by a Shapiro–Wilk test using the shapiro.test function in R to test for normality of the ANOVA residuals. Due to their nonnormality, a Welch one-way test was subsequently performed using the oneway.test function in R. Differences between group pairs were tested using a pairwise Mann–Whitney U test using the pairwise.wilcox.test function in R, controlling for multiple testing using a Benjamini–Hochberg correction.

4.7 | Genotype–Environment Association Analysis

A redundancy analysis (RDA) was used to detect genotype–environment associations and identify putative targets of natural selection in the Bouraké B2 site. RDA has consistently shown a combination of low false positive and high true positive rates, and a power to reveal signals of environmental selection even when they are weak or multilocus, making it the ideal genotype–environment association method for our kind of data (Capblancq et al. 2018; Capblancq and Forester 2021; Forester et al. 2018). We used the environmental dataset from Maggioni et al. (Maggioni et al. 2021), which contained data on temperature, pH, dissolved oxygen, salinity, nutrients (nitrogen oxide [NO_x], orthosilicic acid [Si(OH)₄], phosphate [PO₄]³⁻, and ammonium [NH₄]⁺) and organic and inorganic matter (dissolved inorganic carbon [DIC], particulate organic carbon [POC], and particulate organic nitrogen [PON]) collected from the three study sites between 2017 and 2020. Overall averages and standard deviations were calculated for each variable. In addition, in order to account for the daily variability, for the variables with multiple measurements per day and data from several days (temperature, pH, dissolved oxygen, and salinity) the daily difference between the maximum and minimum daily value was calculated, followed by the average and standard deviation

across days. The resulting environmental matrix contained 30 highly correlated variables, which were summarized into two independent environmental principal components using the “prcomp” R function. The first environmental principal component (ePC1) separated the Bouraké B2 site from the two control sites, explaining 71.7% of the total environmental variance, while the second environmental principal component (ePC2) differentiated the two control sites, explaining 28.3% of the total variance (Figure 2a).

For the genotype data, we used the complete SNP dataset containing 7,894,070 SNPs. First, missing genotypes were imputed with the most common genotype at each site. Then, the “rda” function of the vegan (v.2.6–2) R package (Dixon 2003) was run using the imputed SNP dataset and the ePC1 as the only explanatory variable to detect genotypes associated with the environmental variables that characterize the Bouraké B2 site. Due to the lack of genome-wide genetic structure (Figure 2d), no covariables were considered in the RDA. SNP loadings were extracted for the RDA axis one, and the outlier threshold was established as four times the standard deviation, a highly conservative threshold to identify only those loci under very strong selection in the Bouraké site and minimize false positives (Forester et al. 2018). This resulted in a total of 89 candidate adaptive SNPs, which were annotated using SnpEff (Cingolani et al. 2012) and the annotations from the *A. kenti* reference genome (Cooke et al. 2020).

To investigate the potential function of the candidate adaptive SNPs, Gene Ontology (GO) and KEGG enrichment analyses were performed in the clusterProfiler (v.4.4.4) (Yu et al. 2012) using the annotations from the *A. kenti* reference genome (Cooke et al. 2020). In detail, (1) all *A. kenti* genes with GO terms and KEGG terms were used to create an OrgDb object as the background annotation. (2) Genes with adaptive SNPs were used as the input data set, and then GO and KEGG pathways were enriched using “enrichGO()” and “enricher()” functions, respectively. (3) The calculated *p* values were corrected using the Benjamini–Hochberg procedure. (4) A corrected *p* value of ≤ 0.05 and a *q*-value of ≤ 0.05 were defined as the significance thresholds.

4.8 | 3D Structure Protein Models

3D structure protein models of the two main targets of natural selection in Bouraké were predicted with AlphaFold2 (Jumper et al. 2021) to infer whether the identified missense mutations caused a relevant structural change in the modeled proteins. Although these results are computationally inferred protein structures and need experimental validation, AlphaFold has demonstrated its exceptional accuracy in inferring protein structures, representing a breakthrough in the field of Structural Biology (Varadi et al. 2022; Yang et al. 2023). Moreover, previous studies demonstrated the power of AlphaFold models to predict the structural effects of missense mutations in the human proteome (Cheng et al. 2023). AlphaFold2 was run using the Google ColabFold v.1.5.5 server with default parameters, which uses a deep learning method based on neural network architectures to predict 3D protein structures with high accuracy at the atomic level. Four AlphaFold2 runs were completed in total: TRPA1

reference, TRPA1 mutated, ABCC4 reference, and ABCC4 mutated. For TRPA1, we predicted the protein 3D structure of a single monomer of the tetramer active protein. For each protein, the two models were compared using the structure comparison tool within the Swiss Model (Bienert et al. 2017) (<https://swissmodel.expasy.org/comparison/>). There, plots were generated for each comparison, and structural and interatomic consistencies were calculated using default parameters.

4.9 | Deviations From Hardy–Weinberg Equilibrium (HWE) in the TRPA1 Gene

Deviations from HWE were tested in the nine SNPs with signals of environmental filtering in one of the main targets of selection in Bouraké, the TRPA1 gene. The expected genotype frequencies under HWE were calculated from the observed genotype frequencies (Edwards 2008). Statistical deviations from the expected frequencies under HWE were tested using the “HWEAlltests” function in the HardyWeinberg R package (Graffelman 2015) and graphically represented as a ternary plot using the “HWTernaryPlot” function in the HardyWeinberg package.

4.10 | Symbiodiniaceae Profiles

Fasta files from the ITS2 metabarcoding libraries were submitted to the online SymPortal framework (Hume et al. 2019) (<https://symportal.org>) to generate ITS2 type profiles, representative of phylogenetic resolutions within Symbiodiniaceae, which were plotted in ggplot2. The ITS2 is a multicopy marker, which complicates the differentiation between intragenomic and intergenomic variability (Hume et al. 2019). However, the SymPortal approach is able to identify within-sample informative intragenomic sequences and define ITS2-type profiles representative of putative Symbiodiniaceae taxa (Hume et al. 2019). Further multivariate analyses of symbiont communities were carried out using the ITS2 sequence data. A nonparametric multidimensional scaling (NMDS) analysis was performed using a Wisconsin 4th square root double standardization of the raw data and calculating Bray-Curtis distances among coral colonies using the vegan R package. This standardization was used to reduce the influence of rare and common Symbiodiniaceae sequences, as it standardizes sequences by their maxima and then relativizes them by site totals (Bray and Curtis 1957). Subsequently, a simpler analysis was run on the standardized data using the sampling sites as a grouping to identify the Symbiodiniaceae sequences that contribute the most to the dissimilarity between sampling sites, using the “simpler” function in vegan. Plots were generated using ggplot2.

Author Contributions

Carlos Leiva: data curation, formal analysis, investigation, methodology, visualization, writing – original draft, writing – review and editing. **Gergely Torda:** conceptualization, data curation, formal analysis, funding acquisition, investigation, methodology, visualization, writing – original draft, writing – review and editing. **Chengran Zhou:** conceptualization, data curation, formal analysis, investigation, methodology, visualization, writing – original draft, writing – review and

editing. **Yunrui Pan:** formal analysis, visualization, writing – review and editing. **Jess Harris:** methodology, writing – review and editing. **Xueyan Xiang:** methodology, writing – review and editing. **Shangjin Tan:** methodology, writing – review and editing. **Wei Tian:** methodology, writing – review and editing. **Benjamin Hume:** methodology, writing – review and editing. **David J. Miller:** supervision, writing – review and editing. **Qiye Li:** methodology, supervision, writing – review and editing. **Guojie Zhang:** conceptualization, methodology, supervision, writing – review and editing. **Ira Cooke:** conceptualization, data curation, investigation, methodology, supervision, visualization, writing – review and editing. **Riccardo Rodolfo-Metalpa:** conceptualization, funding acquisition, supervision, writing – review and editing.

Acknowledgments

We thank Dr. Misha Matz, Dr. Tong Wei, and Dr. Eugenia Almacellas for the many inspiring discussions. This study contributes to the ICONA International CO₂ Natural Analogues Network.

Conflicts of Interest

The authors declare no conflicts of interest.

Data Availability Statement

The data that support the findings of this study are openly available in the following public repositories: coral host genomic reads are openly available in the NCBI SRA database BioProject ID PRJNA1186808; Symbiodiniaceae amplicon sequencing reads are openly available in the NCBI SRA database BioProject ID PRJNA1222880; the SNPs dataset in Zenodo at <https://doi.org/10.5281/zenodo.12699822>; the environmental matrix in Zenodo at <https://doi.org/10.5281/zenodo.14843759>; the diameter and color data for each coral colony in Zenodo at <https://doi.org/10.5281/zenodo.14858579>.

References

- Abrego, D., K. E. Ulstrup, B. L. Willis, and M. J. H. van Oppen. 2008. “Species-Specific Interactions Between Algal Endosymbionts and Coral Hosts Define Their Bleaching Response to Heat and Light Stress.” *Proceedings of the Royal Society B: Biological Sciences* 275, no. 1648: 2273–2282. <https://doi.org/10.1098/rspb.2008.0180>.
- Aidoo, M., D. J. Terlouw, M. S. Kolczak, et al. 2002. “Protective Effects of the Sickle Cell Gene Against Malaria Morbidity and Mortality.” *Lancet* 359, no. 9314: 1311–1312. [https://doi.org/10.1016/S0140-6736\(02\)08273-9](https://doi.org/10.1016/S0140-6736(02)08273-9).
- Alessi, C., H. Lemonnier, E. F. Camp, N. Wabete, C. Payri, and R. Rodolfo Metalpa. 2024. “Algal Symbiont Diversity in Acropora Muricata From the Extreme Reef of Bouraké Associated With Resistance to Coral Bleaching.” *PLoS One* 19, no. 2: e0296902. <https://doi.org/10.1371/journal.pone.0296902>.
- Alexander, D. H., J. Novembre, and K. Lange. 2009. “Fast Model-Based Estimation of Ancestry in Unrelated Individuals.” *Genome Research* 19, no. 9: 1655–1664. <https://doi.org/10.1101/gr.094052.109>.
- Alonge, M., L. Lebeigle, M. Kirsche, et al. 2022. “Automated Assembly Scaffolding Using RagTag Elevates a New Tomato System for High-Throughput Genome Editing.” *Genome Biology* 23, no. 1: 258. <https://doi.org/10.1186/s13059-022-02823-7>.
- Anthony, K. R. N. 2016. “Coral Reefs Under Climate Change and Ocean Acidification: Challenges and Opportunities for Management and Policy.” *Annual Review of Environment and Resources* 41, no. 1: 59–81. <https://doi.org/10.1146/annurev-environ-110615-085610>.
- Bailey, S. F., L. A. Alonso Morales, and R. Kassen. 2021. “Effects of Synonymous Mutations Beyond Codon Bias: The Evidence for Adaptive Synonymous Substitutions From Microbial Evolution Experiments.” *Genome Biology and Evolution* 13, no. 9: evab141. <https://doi.org/10.1093/gbe/evab141>.

- Baker, A. C., C. J. Starger, T. R. McClanahan, and P. W. Glynn. 2004. "Corals' Adaptive Response to Climate Change." *Nature* 430, no. 7001: 741. <https://doi.org/10.1038/430741a>.
- Bay, R. A., and S. R. Palumbi. 2014. "Multilocus Adaptation Associated With Heat Resistance in Reef-Building Corals." *Current Biology* 24, no. 24: 2952–2956.
- Berkelmans, R., and M. J. H. van Oppen. 2006. "The Role of Zooxanthellae in the Thermal Tolerance of Corals: A 'Nugget of Hope' for Coral Reefs in an Era of Climate Change." *Proceedings of the Royal Society B: Biological Sciences* 273, no. 1599: 2305–2312. <https://doi.org/10.1098/rspb.2006.3567>.
- Bertucci, A., S. Forêt, E. E. Ball, and D. J. Miller. 2015. "Transcriptomic Differences Between Day and Night in *Acropora millepora* Provide New Insights Into Metabolite Exchange and Light-Enhanced Calcification in Corals." *Molecular Ecology* 24, no. 17: 4489–4504. <https://doi.org/10.1111/mec.13328>.
- Bienert, S., A. Waterhouse, T. A. P. de Beer, et al. 2017. "The SWISS-MODEL Repository—New Features and Functionality." *Nucleic Acids Research* 45, no. D1: D313–D319. <https://doi.org/10.1093/nar/gkw1132>.
- Bitarello, B. D., D. Y. C. Brandt, D. Meyer, and A. M. Andrés. 2023. "Inferring Balancing Selection From Genome-Scale Data." *Genome Biology and Evolution* 15, no. 3: evad032. <https://doi.org/10.1093/gbe/evad032>.
- Boag, P. T., and P. R. Grant. 1981. "Intense Natural Selection in a Population of Darwin's Finches (Geospizinae) in the Galápagos." *Science* 214, no. 4516: 82–85. <https://doi.org/10.1126/science.214.4516.82>.
- Bray, J. R., and J. T. Curtis. 1957. "An Ordination of the Upland Forest Communities of Southern Wisconsin." *Ecological Monographs* 27, no. 4: 325–349. <https://doi.org/10.2307/1942268>.
- Bridge, T. C. L., P. F. Cowman, A. M. Quattrini, et al. 2024. "A Tenuis Relationship: Traditional Taxonomy Obscures Systematics and Biogeography of the '*Acropora tenuis*' (Scleractinia: Acroporidae) Species Complex." *Zoological Journal of the Linnean Society* 202, no. 1: zlad062. <https://doi.org/10.1093/zoolinnean/zlad062>.
- Calvin, K., D. Dasgupta, G. Krinner, et al. 2023. *IPCC, 2023: Climate Change 2023: Synthesis Report. Contribution of Working Groups I, II and III to the Sixth Assessment Report of the Intergovernmental Panel on Climate Change*, edited by Core Writing Team, H. Lee, and J. Romero, 1st ed. Intergovernmental Panel on Climate Change (IPCC). <https://doi.org/10.59327/IPCC/AR6-9789291691647>.
- Camp, E. F., M. R. Nitschke, R. Rodolfo-Metalpa, et al. 2017. "Reef-Building Corals Thrive Within Hot-Acidified and Deoxygenated Waters." *Scientific Reports* 7, no. 1: 2434. <https://doi.org/10.1038/s41598-017-02383-y>.
- Camp, E. F., V. Schoepf, P. J. Mumby, et al. 2018. "The Future of Coral Reefs Subject to Rapid Climate Change: Lessons From Natural Extreme Environments." *Frontiers in Marine Science* 5: 00004. <https://doi.org/10.3389/fmars.2018.00004>.
- Camp, E. F., D. J. Suggett, C. Pogoreutz, et al. 2020. "Corals Exhibit Distinct Patterns of Microbial Reorganisation to Thrive in an Extreme Inshore Environment." *Coral Reefs* 39, no. 3: 701–716. <https://doi.org/10.1007/s00338-019-01889-3>.
- Campbell-Staton, S. C., Z. A. Cheviron, N. Rochette, J. Catchen, J. B. Losos, and S. V. Edwards. 2017. "Winter Storms Drive Rapid Phenotypic, Regulatory, and Genomic Shifts in the Green Anole Lizard." *Science* 357, no. 6350: 495–498. <https://doi.org/10.1126/science.aam5512>.
- Cantin, N. E., M. J. H. van Oppen, B. L. Willis, J. C. Mieog, and A. P. Negri. 2009. "Juvenile Corals Can Acquire More Carbon From High-Performance Algal Symbionts." *Coral Reefs* 28, no. 2: 405–414. <https://doi.org/10.1007/s00338-009-0478-8>.
- Capblancq, T., and B. R. Forester. 2021. "Redundancy Analysis: A Swiss Army Knife for Landscape Genomics." *Methods in Ecology and Evolution* 12, no. 12: 2298–2309. <https://doi.org/10.1111/2041-210X.13722>.
- Capblancq, T., K. Luu, M. G. B. Blum, and E. Bazin. 2018. "Evaluation of Redundancy Analysis to Identify Signatures of Local Adaptation." *Molecular Ecology Resources* 18, no. 6: 1223–1233. <https://doi.org/10.1111/1755-0998.12906>.
- Chang, C. C., C. C. Chow, L. C. Tellier, S. Vattikuti, S. M. Purcell, and J. J. Lee. 2015. "Second-Generation PLINK: Rising to the Challenge of Larger and Richer Datasets." *GigaScience* 4, no. 1: 7. <https://doi.org/10.1186/s13742-015-0047-8>.
- Charlesworth, B. 2009. "Effective Population Size and Patterns of Molecular Evolution and Variation." *Nature Reviews Genetics* 10, no. 3: 195–205. <https://doi.org/10.1038/nrg2526>.
- Chen, Y., Y. Chen, C. Shi, et al. 2018. "SOAPnuke: A MapReduce Acceleration-Supported Software for Integrated Quality Control and Preprocessing of High-Throughput Sequencing Data." *GigaScience* 7, no. 1: 1–6. <https://doi.org/10.1093/gigascience/gix120>.
- Cheng, J., G. Novati, J. Pan, et al. 2023. "Accurate Proteome-Wide Missense Variant Effect Prediction With AlphaMissense." *Science* 381, no. 6664: adg7492. <https://doi.org/10.1126/science.adg7492>.
- Cingolani, P., A. Platts, L. L. Wang, et al. 2012. "A Program for Annotating and Predicting the Effects of Single Nucleotide Polymorphisms, SnpEff: SNPs in the Genome of *Drosophila melanogaster* Strain w1118; Iso-2; Iso-3." *Fly* 6, no. 2: 80–92.
- Connell, J. H. 1978. "Diversity in Tropical Rain Forests and Coral Reefs: High Diversity of Trees and Corals Is Maintained Only in a Nonequilibrium State." *Science* 199, no. 4335: 1302–1310. <https://doi.org/10.1126/science.199.4335.1302>.
- Cooke, I., H. Ying, S. Forêt, et al. 2020. "Genomic Signatures in the Coral Holobiont Reveal Host Adaptations Driven by Holocene Climate Change and Reef Specific Symbionts." *Science Advances* 6, no. 48: eabc6318.
- Costanza, R., R. de Groot, P. Sutton, et al. 2014. "Changes in the Global Value of Ecosystem Services." *Global Environmental Change* 26: 152–158. <https://doi.org/10.1016/j.gloenvcha.2014.04.002>.
- Danecek, P., A. Auton, G. Abecasis, et al. 2011. "The Variant Call Format and VCFtools." *Bioinformatics* 27, no. 15: 2156–2158. <https://doi.org/10.1093/bioinformatics/btr330>.
- Danecek, P., J. K. Bonfield, J. Liddle, et al. 2021. "Twelve Years of SAMtools and BCFtools." *GigaScience* 10, no. 2: giab008.
- Davies, S. W., E. A. Trembl, C. D. Kenkel, and M. V. Matz. 2015. "Exploring the Role of Micronesian Islands in the Maintenance of Coral Genetic Diversity in the Pacific Ocean." *Molecular Ecology* 24, no. 1: 70–82. <https://doi.org/10.1111/mec.13005>.
- Detournay, O., and V. M. Weis. 2011. "Role of the Sphingosine Rheostat in the Regulation of Cnidarian-Dinoflagellate Symbioses." *Biological Bulletin* 221, no. 3: 261–269. <https://doi.org/10.1086/BBLv221n3p261>.
- Dixon, P. 2003. "VEGAN, a Package of R Functions for Community Ecology." *Journal of Vegetation Science* 14, no. 6: 927–930.
- Edwards, A. W. F. 2008. "G. H. Hardy (1908) and Hardy–Weinberg Equilibrium." *Genetics* 179, no. 3: 1143–1150. <https://doi.org/10.1534/genetics.104.92940>.
- Forester, B. R., J. R. Lasky, H. H. Wagner, and D. L. Urban. 2018. "Comparing Methods for Detecting Multilocus Adaptation With Multivariate Genotype–Environment Associations." *Molecular Ecology* 27, no. 9: 2215–2233. <https://doi.org/10.1111/mec.14584>.
- Frichot, E., and O. François. 2015. "LEA: An R Package for Landscape and Ecological Association Studies." *Methods in Ecology and Evolution* 6, no. 8: 925–929. <https://doi.org/10.1111/2041-210X.12382>.
- Fuller, Z. L., V. J. Mocellin, L. A. Morris, et al. 2020. "Population Genetics of the Coral *Acropora millepora*: Toward Genomic Prediction of Bleaching." *Science* 369, no. 6501: eaba4674.
- Goldstone, J. V. 2008. "Environmental Sensing and Response Genes in Cnidaria: The Chemical Defensome in the Sea Anemone *Nematostella*

- vectensis." *Cell Biology and Toxicology* 24, no. 6: 483–502. <https://doi.org/10.1007/s10565-008-9107-5>.
- González-Delgado, S., O. S. Wangenstein, C. Sangil, et al. 2023. "High Taxonomic Diversity and Miniaturization in Benthic Communities Under Persistent Natural CO₂ Disturbances." *Proceedings of the Royal Society B: Biological Sciences* 290, no. 1995: 22417. <https://doi.org/10.1098/rspb.2022.2417>.
- Graffelman, J. 2015. "Exploring Diallelic Genetic Markers: The HardyWeinberg Package." *Journal of Statistical Software* 64, no. 3: 1–23. <https://doi.org/10.18637/jss.v064.i03>.
- He, C., T. Han, W. Huang, et al. 2024. "Deciphering Omics Atlases to Aid Stony Corals in Response to Global Change." <https://doi.org/10.21203/rs.3.rs-4037544/v1>.
- Huang, J., X. Liang, Y. Xuan, et al. 2017. "A Reference Human Genome Dataset of the BGISEQ-500 Sequencer." *GigaScience* 6, no. 5: 1–9. <https://doi.org/10.1093/gigascience/gix024>.
- Hughes, T. P., J. T. Kerry, A. H. Baird, et al. 2018. "Global Warming Transforms Coral Reef Assemblages." *Nature* 556, no. 7702: 492–496. <https://doi.org/10.1038/s41586-018-0041-2>.
- Hume, B. C. C., E. G. Smith, M. Ziegler, et al. 2019. "SymPortal: A Novel Analytical Framework and Platform for Coral Algal Symbiont Next-Generation Sequencing ITS2 Profiling." *Molecular Ecology Resources* 19, no. 4: 1063–1080. <https://doi.org/10.1111/1755-0998.13004>.
- Hume, B. C. C., C. R. Voolstra, C. Arif, et al. 2016. "Ancestral Genetic Diversity Associated With the Rapid Spread of Stress-Tolerant Coral Symbionts in Response to Holocene Climate Change." *Proceedings of the National Academy of Sciences* 113, no. 16: 4416–4421. <https://doi.org/10.1073/pnas.1601910113>.
- Hume, B. C. C., M. Ziegler, J. Poulain, et al. 2018. "An Improved Primer Set and Amplification Protocol With Increased Specificity and Sensitivity Targeting the Symbiodinium ITS2 Region." *PeerJ* 6: e4816. <https://doi.org/10.7717/peerj.4816>.
- Jombart, T. 2008. "Adegenet: A R Package for the Multivariate Analysis of Genetic Markers." *Bioinformatics* 24, no. 11: 1403–1405.
- Jumper, J., R. Evans, A. Pritzel, et al. 2021. "Highly Accurate Protein Structure Prediction With AlphaFold." *Nature* 596, no. 7873: 583–589. <https://doi.org/10.1038/s41586-021-03819-2>.
- Katoh, K. 2002. "MAFFT: A Novel Method for Rapid Multiple Sequence Alignment Based on Fast Fourier Transform." *Nucleic Acids Research* 30, no. 14: 3059–3066. <https://doi.org/10.1093/nar/gkf436>.
- Kenkel, C. D., A. Moya, J. Strahl, C. Humphrey, and L. K. Bay. 2018. "Functional Genomic Analysis of Corals From Natural CO₂-Seeps Reveals Core Molecular Responses Involved in Acclimatization to Ocean Acidification." *Global Change Biology* 24, no. 1: 158–171.
- Khatri, B. S., and A. Burt. 2019. "Robust Estimation of Recent Effective Population Size From Number of Independent Origins in Soft Sweeps." *Molecular Biology and Evolution* 36, no. 9: 2040–2052. <https://doi.org/10.1093/molbev/msz081>.
- Kitchen, S. A., and V. M. Weis. 2017. "The Sphingosine Rheostat Is Involved in the Cnidarian Heat Stress Response but Not Necessarily in Bleaching." *Journal of Experimental Biology* 220, no. 9: jeb.153858. <https://doi.org/10.1242/jeb.153858>.
- Knaus, B. J., and N. J. Grünwald. 2017. "Vcfr: A Package to Manipulate and Visualize Variant Call Format Data in R." *Molecular Ecology Resources* 17, no. 1: 44–53. <https://doi.org/10.1111/1755-0998.12549>.
- Knowlton, N., R. E. Brainard, R. Fisher, M. Moews, L. Plaisance, and M. J. Caley. 2010. "Coral Reef Biodiversity." In *Coral Reef Biodiversity*, 65–74. Life in the World's Oceans.
- Leiva, C., R. Pérez-Portela, and S. Lemer. 2023. "Genomic Signatures Suggesting Adaptation to Ocean Acidification in a Coral Holobiont From Volcanic CO₂ Seeps." *Communications Biology* 6, no. 1: 769. <https://doi.org/10.1038/s42003-023-05103-7>.
- Letunic, I., and P. Bork. 2021. "Interactive Tree of Life (iTOL) v5: An Online Tool for Phylogenetic Tree Display and Annotation." *Nucleic Acids Research* 49, no. W1: W293–W296. <https://doi.org/10.1093/nar/gkab301>.
- Maggioni, F., M. Pujo-Pay, J. Aucan, et al. 2021. "The Bouraké Semi-Enclosed Lagoon (New Caledonia)—A Natural Laboratory to Study the Lifelong Adaptation of a Coral Reef Ecosystem to Extreme Environmental Conditions." *Biogeosciences* 18, no. 18: 5117–5140. <https://doi.org/10.5194/bg-18-5117-2021>.
- Manichaikul, A., J. C. Mychaleckyj, S. S. Rich, K. Daly, M. Sale, and W.-M. Chen. 2010. "Robust Relationship Inference in Genome-Wide Association Studies." *Bioinformatics* 26, no. 22: 2867–2873. <https://doi.org/10.1093/bioinformatics/btq559>.
- McGinty, E. S., J. Pieczonka, and L. D. Mydlarz. 2012. "Variations in Reactive Oxygen Release and Antioxidant Activity in Multiple Symbiodinium Types in Response to Elevated Temperature." *Microbial Ecology* 64, no. 4: 1000–1007. <https://doi.org/10.1007/s00248-012-0085-z>.
- Minh, B. Q., H. A. Schmidt, O. Chernomor, et al. 2020. "IQ-TREE 2: New Models and Efficient Methods for Phylogenetic Inference in the Genomic Era." *Molecular Biology and Evolution* 37, no. 5: 1530–1534. <https://doi.org/10.1093/molbev/msaa015>.
- Mohamed, A. R., V. Cumbo, S. Harii, et al. 2016. "The Transcriptomic Response of the Coral *Acropora digitifera* to a Competent Symbiodinium Strain: The Symbiosome as an Arrested Early Phagosome." *Molecular Ecology* 25, no. 13: 3127–3141.
- Mori, Y., N. Takahashi, T. Kurokawa, and S. Kiyonaka. 2017. "TRP Channels in Oxygen Physiology: Distinctive Functional Properties and Roles of TRPA1 in O₂ Sensing." *Proceedings of the Japan Academy, Series B* 93, no. 7: 464–482. <https://doi.org/10.2183/pjab.93.028>.
- Ortiz, E. M. 2019. vcf2phylip v2.0: Convert a VCF Matrix into Several Matrix Formats for Phylogenetic Analysis (Version v2.0) [Computer Software]. [Object Object]. <https://doi.org/10.5281/ZENODO.2540861>.
- Ortiz, J. C., R. J. Pears, R. Beeden, et al. 2021. "Important Ecosystem Function, Low Redundancy and High Vulnerability: The Trifecta Argument for Protecting the Great Barrier Reef's Tabular Acropora." *Conservation Letters* 14, no. 5: e12817. <https://doi.org/10.1111/conl.12817>.
- Peng, G., X. Shi, and T. Kadowaki. 2015. "Evolution of TRP Channels Inferred by Their Classification in Diverse Animal Species." *Molecular Phylogenetics and Evolution* 84: 145–157. <https://doi.org/10.1016/j.ympev.2014.06.016>.
- Prada, C., B. Hanna, A. F. Budd, et al. 2016. "Empty Niches After Extinctions Increase Population Sizes of Modern Corals." *Current Biology* 26, no. 23: 3190–3194. <https://doi.org/10.1016/j.cub.2016.09.039>.
- Quigley, K. M., L. K. Bay, and B. L. Willis. 2017. "Temperature and Water Quality-Related Patterns in Sediment-Associated Symbiodinium Communities Impact Symbiont Uptake and Fitness of Juveniles in the Genus *Acropora*." *Frontiers in Marine Science* 4: 401. <https://doi.org/10.3389/fmars.2017.00401>.
- Quinlan, A. R., and I. M. Hall. 2010. "BEDTools: A Flexible Suite of Utilities for Comparing Genomic Features." *Bioinformatics* 26, no. 6: 841–842. <https://doi.org/10.1093/bioinformatics/btq033>.
- Rubin, E. T., I. C. Enochs, C. Foord, et al. 2021. "Molecular Mechanisms of Coral Persistence Within Highly Urbanized Locations in the Port of Miami, Florida." *Frontiers in Marine Science* 8: 695236. <https://doi.org/10.3389/fmars.2021.695236>.
- Russo, V. 2019. *The Role of TRP Receptors in the Signalling Pathways in Hydra Vulgaris*. Università Degli Studi Roma Tre.

- Samad, A., L. Sura, J. Benedikt, et al. 2011. "The C-Terminal Basic Residues Contribute to the Chemical- and Voltage-Dependent Activation of TRPA1." *Biochemical Journal* 433, no. 1: 197–204. <https://doi.org/10.1042/BJ20101256>.
- Santiago, E., I. Novo, A. F. Pardiñas, M. Saura, J. Wang, and A. Caballero. 2020. "Recent Demographic History Inferred by High-Resolution Analysis of Linkage Disequilibrium." *Molecular Biology and Evolution* 37, no. 12: 3642–3653. <https://doi.org/10.1093/molbev/msaa169>.
- Saura, M., A. Caballero, E. Santiago, et al. 2021. "Estimates of Recent and Historical Effective Population Size in Turbot, Seabream, Seabass and Carp Selective Breeding Programmes." *Genetics Selection Evolution* 53, no. 1: 85. <https://doi.org/10.1186/s12711-021-00680-9>.
- Scucchia, F., P. Zaslansky, C. Boote, A. Doheny, T. Mass, and E. F. Camp. 2023. "The Role and Risks of Selective Adaptation in Extreme Coral Habitats." *Nature Communications* 14, no. 1: 4475. <https://doi.org/10.1038/s41467-023-39651-7>.
- Shinzato, C., K. Khalturin, J. Inoue, et al. 2021. "Eighteen Coral Genomes Reveal the Evolutionary Origin of Acropora Strategies to Accommodate Environmental Changes." *Molecular Biology and Evolution* 38, no. 1: 16–30. <https://doi.org/10.1093/molbev/msaa216>.
- Sing Wong, A., S. Vrontos, and M. L. Taylor. 2022. "An Assessment of People Living by Coral Reefs Over Space and Time." *Global Change Biology* 28, no. 23: 7139–7153. <https://doi.org/10.1111/gcb.16391>.
- Smith, E. G., K. M. Hazzouri, J. Y. Choi, et al. 2022. "Signatures of Selection Underpinning Rapid Coral Adaptation to the world's Warmest Reefs. Science." *Advances* 8, no. 2: eabl7287. <https://doi.org/10.1126/sciadv.abl7287>.
- Sork, V. L. 2016. "Gene Flow and Natural Selection Shape Spatial Patterns of Genes in Tree Populations: Implications for Evolutionary Processes and Applications." *Evolutionary Applications* 9, no. 1: 291–310. <https://doi.org/10.1111/eva.12316>.
- Tamura, K., G. Stecher, D. Peterson, A. Filipski, and S. Kumar. 2013. "MEGA6: Molecular Evolutionary Genetics Analysis Version 6.0." *Molecular Biology and Evolution* 30, no. 12: 2725–2729. <https://doi.org/10.1093/molbev/mst197>.
- Tanvet, C., F. Benzoni, C. Peignon, G. Thouzeau, and R. Rodolfo-Metalpa. 2022. "High Coral Recruitment Despite Coralline Algal Loss Under Extreme Environmental Conditions." *Frontiers in Marine Science* 9: 837877. <https://doi.org/10.3389/fmars.2022.837877>.
- Tanvet, C., E. F. Camp, J. Sutton, F. Houlbrèque, G. Thouzeau, and R. Rodolfo-Metalpa. 2023. "Corals Adapted to Extreme and Fluctuating Seawater pH Increase Calcification Rates and Have Unique Symbiont Communities." *Ecology and Evolution* 13, no. 5: e10099.
- Thomas, L., N. H. Rose, R. A. Bay, et al. 2018. "Mechanisms of Thermal Tolerance in Reef-Building Corals Across a Fine-Grained Environmental Mosaic: Lessons From Ofu, American Samoa." *Frontiers in Marine Science* 4: 434. <https://doi.org/10.3389/fmars.2017.00434>.
- Thomas, L., J. N. Underwood, N. H. Rose, et al. 2022. "Spatially Varying Selection Between Habitats Drives Physiological Shifts and Local Adaptation in a Broadcast Spawning Coral on a Remote Atoll in Western Australia. Science." *Advances* 8, no. 17: eabl9185. <https://doi.org/10.1126/sciadv.abl9185>.
- Torda, G., J. M. Donelson, M. Aranda, et al. 2017. "Rapid Adaptive Responses to Climate Change in Corals." *Nature Climate Change* 7, no. 9: 627–636.
- Varadi, M., S. Anyango, M. Deshpande, et al. 2022. "AlphaFold Protein Structure Database: Massively Expanding the Structural Coverage of Protein-Sequence Space With High-Accuracy Models." *Nucleic Acids Research* 50, no. D1: D439–D444. <https://doi.org/10.1093/nar/gkab1061>.
- Wang, J., E. Santiago, and A. Caballero. 2016. "Prediction and Estimation of Effective Population Size." *Heredity* 117, no. 4: 193–206. <https://doi.org/10.1038/hdy.2016.43>.
- Wickham, H., and H. Wickham. 2016. *Data Analysis*. Springer.
- Wilson, K., Y. Li, V. Whan, et al. 2002. "Genetic Mapping of the Black Tiger Shrimp *Penaeus monodon* With Amplified Fragment Length Polymorphism." *Aquaculture* 204, no. 3–4: 297–309. [https://doi.org/10.1016/S0044-8486\(01\)00842-0](https://doi.org/10.1016/S0044-8486(01)00842-0).
- Yang, Z., X. Zeng, Y. Zhao, and R. Chen. 2023. "AlphaFold2 and Its Applications in the Fields of Biology and Medicine." *Signal Transduction and Targeted Therapy* 8, no. 1: 115. <https://doi.org/10.1038/s41392-023-01381-z>.
- Yoshioka, Y., H. Yamashita, G. Suzuki, et al. 2021. "Whole-Genome Transcriptome Analyses of Native Symbionts Reveal Host Coral Genomic Novelty for Establishing Coral-Algae Symbioses." *Genome Biology and Evolution* 13, no. 1: evaa240. <https://doi.org/10.1093/gbe/evaa240>.
- Yu, G., L.-G. Wang, Y. Han, and Q.-Y. He. 2012. "clusterProfiler: An R Package for Comparing Biological Themes Among Gene Clusters." *OMICS: A Journal of Integrative Biology* 16, no. 5: 284–287. <https://doi.org/10.1089/omi.2011.0118>.
- Zhang, J., Z. T. Richards, A. A. S. Adam, et al. 2022. "Evolutionary Responses of a Reef-Building Coral to Climate Change at the End of the Last Glacial Maximum." *Molecular Biology and Evolution* 39, no. 10: msac201. <https://doi.org/10.1093/molbev/msac201>.
- Zhang, J., N. M. Schneller, M. A. Field, et al. 2024. "Chromosomal Inversions Harbour Excess Mutational Load in the Coral, Acropora Kenti, on the Great Barrier Reef." *Molecular Ecology* 33, no. 16: e17468. <https://doi.org/10.1111/mec.17468>.
- Zhao, J., J. V. Lin King, C. E. Paulsen, Y. Cheng, and D. Julius. 2020. "Irritant-Evoked Activation and Calcium Modulation of the TRPA1 Receptor." *Nature* 585, no. 7823: 141–145. <https://doi.org/10.1038/s41586-020-2480-9>.
- Zheng, X., D. Levine, J. Shen, S. M. Gogarten, C. Laurie, and B. S. Weir. 2012. "A High-Performance Computing Toolset for Relatedness and Principal Component Analysis of SNP Data." *Bioinformatics* 28, no. 24: 3326–3328. <https://doi.org/10.1093/bioinformatics/bts606>.

Supporting Information

Additional supporting information can be found online in the Supporting Information section.